Lithium-pyrazole-3,4,5-tricarbonitrile: Ion Pairing and Lithium Ion Affinity Studies

Henrik Markusson,*,† Stéphane Béranger,‡ Patrik Johansson,† Michel Armand,‡ and Per Jacobsson†

Department of Applied Physics, Chalmers University of Technology, SE-412 96 Göteborg, Sweden, and Département de Chimie, Université de Montréal, CP. 6128 Succursale Centre Ville, Montreal, QC, Canada H3C 3J7

Received: June 30, 2003; In Final Form: September 4, 2003

Negative charge stabilized by ring delocalization on five-membered rings is a practical and theoretically interesting alternative to conventional fluorine-based anions. Coordination of the lithium cation to the pyrazole-3,4,5-tricarbonitrile (PATC) anion was studied using vibrational spectroscopy (Raman and IR) and ab initio SCF-MO Hartree−Fock (HF) calculations. Four 1:1 ion pair geometries were found, one being energetically more stable. By comparing theoretical spectra with both IR and Raman spectra of salt solutions, it was found that the lithium ion favors bidentate coordination to the ring nitrogen atoms, as suggested by the binding energies. Finally, comparisons were made with previously calculated coordination strengths for other similar lithium anion 1:1 systems.

Introduction

The field of ion dissociation in aprotic media has been mainly overlooked until recent years. The necessity of having a weakly coordinating anion is, however, paramount, with applications in electrolytes (liquid and solid) and catalysis. Only a handful of anions are known to fulfill the "weakly coordinating" criterion (ClO_4^-, BF_4^-, $CF_3SO_3^-$, PF_6^-, and AsF_6^-), but all of these compounds have drawbacks either in terms of safety (ClO_4^-) or toxicity (AsF_6^-). The widely used PF_6^- (e.g., as $LiPF_6$ in lithium ion batteries) is highly unstable; the facile release of PF_5, a strong Lewis acid, induces a cascade of unwanted side reactions and safety problems. The conventional wisdom holds that stable, weakly coordinating anions can only be obtained from the most electronegative elements (F, O, Cl) that are not prone to donate electron pairs. The need for a wider choice of anions initially stemmed from the field of polymer electrolytes.[1] Such materials are obtained by dissolving a salt in a solvating macromolecular media; their end use in large, high energy density batteries is synonymous with nontoxicity and safety. Solvating polymers have low dielectric constants, and thus the importance of dissociation is even more stringent than in other ion-conducting media to reach high conductivity. Besides the intrinsic high interest of polymer electrolytes, they also act as "contrasting agents" to predict dissociation in other aprotic media.

Experimentally, ion pairing can be studied at the molecular level using vibrational spectroscopy[2] and macroscopically by measuring transference numbers for the different species.[3] This should include the diffusion of neutral ion pairs as well. Theoretically, ab initio calculations can provide the theoretical vibrational spectra for different ion pairs and an estimate of the anions' lithium ion affinities.[4−6]

One salt that has been designed specifically for polymer electrolytes and whose applications now far exceed this field is the lithium "imide"/TFSI ($Li[CF_3SO_2)_2N]$). Organofluorine chemicals are, however, expensive and remnant in the environment.[7,8] Our research groups have recently studied a new type of lithium salt where the anion is of the Hückel type (i.e., the charge is stabilized on a five-membered azole ring to which electron-withdrawing carbonitrile groups are attached, and without recourse to electronegative atoms[9]). Oxidation of the first member of this salt family (two nitrile groups) does not take place before 4 V versus Li^+/Li^0 is reached, and in liquid electrolytes, it has ion conductivities on par with those of $LiCF_3SO_3$ and $LiBF_4$.[10] Preliminary investigations of these types of salts by computer simulations has suggested the inception of a new salt, lithium-pyrazole-3,4,5-tricarbonitrile (Li-PATC). This salt has a similar five-membered carbon−nitrogen ring, with three pendant CN groups. We hope that the introduction of the extra CN group will further decrease the lithium ion affinity of the anion.

The only literature found for this lithium salt is on the synthesis of different pyrazole acids.[11,12] Spectroscopic studies are topical, as well as the recent relevant study on the similar triazole (TADC).[9]

In the present study, ab initio calculations of geometries, energies, atomic charges, vibrational frequencies, and Raman and IR intensities are presented for the free anion (PATC) and different Li-PATC 1:1 ion pairs. The calculated data are compared with experimental Raman and IR spectra of the pure salt and DMSO salt solutions.

Methods

Experimental. *Synthesis.* The corresponding acid was prepared by the 1,3 addition of dimethyl acetylene-dicarboxylate on diazo-acetonitrile, as per Weis.[13] The solution of diazo-acetonitrile (*caution: explosive!*) was made according to a modified procedure by Dewar and Pettit, where diethyl ether was replaced by dichloromethane.[14] The sequence of reactions is shown in Scheme 1.

The acid was obtained in pure form through vacuum sublimation. The (yet unknown) lithium salt was prepared by

* Corresponding author. E-mail: henrikn@fy.chalmers.se. Tel: +46 31 772 3352. Fax: +46 31 772 2090.
† Chalmers University of Technology.
‡ Université de Montréal.

10.1021/jp035860r CCC: $25.00
Published on Web 11/01/2003

SCHEME 1: Synthesis Path for Li-PATC

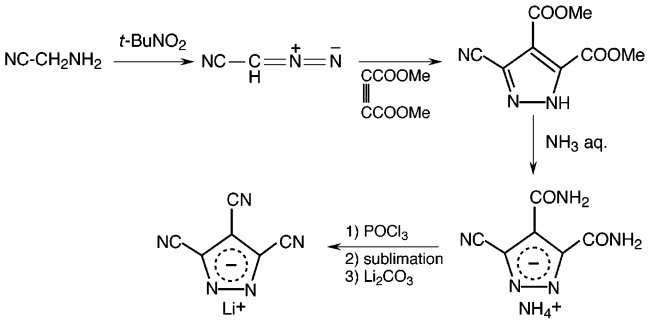

using lithium carbonate (1.5× excess) in methanol at room temperature and then dried. The solid was extracted with acetonitrile. After filtration and the removal of acetonitrile, the salt was left as a white solid. Summary of characterization results: ^{13}C NMR (MeOD, Bruker AV 400, 100.5 MHz): δ 126.62 (s), 116.59 (s), 112.84 (s), 111.98 (s), 110.66 (s), 98.94 (s). MS (FAB−NBA) *m*/*e*: 142 [M], 291 [2M + Li], 440 [3M + 2Li]. T_f 192−194 °C.

Prior to any sample preparation, the salt was dried on a vacuum line (~10^{-2} Torr) for 125 h at 90 °C. All sample preparation was done in an argon-filled drybox. Salt solutions were made by dissolving appropriate amounts of salt in fresh, dry DMSO (Aldrich, AR grade). The salt concentrations varied from 0.3 to 4.0 M, to create solutions with different amounts of "free" anions vs contact ion pairs present. At the highest concentration, the salt solution was saturated.

Raman spectra were recorded at room temperature on a Bruker IFS 66 and an FRA 106 Raman spectrometer equipped with a liquid-nitrogen-cooled enhanced germanium detector and a narrow Rayleigh filter. The laser wavelength was 1.064 μm, and the resolution was set to 2.0 cm^{-1}. The recorded spectra are the results of accumulating and averaging ~12 000 scans for the solutions and ~6000 scans for the dry salt.

FTIR spectra were recorded at room temperature within the drybox with a Bruker 22 (Vektor) spectrometer, equipped with an ATR unit (45° ZnSe prism for solutions and Golden Gate for dry salt, both products of Graseby Specac). Each spectrum is a result of the accumulation of 50 scans. The spectral resolution was set to 2 cm^{-1} in all cases.

For all solution spectra, the intensities were normalized using the ~3000 cm^{-1} carbon−hydrogen stretching vibrations from DMSO. The vibrational peaks were fit by the program PeakFit[15] using a Voigt function. The Lorentzian contribution to the Voigt profile was allowed to vary freely for all peaks, and a shared Gaussian contribution was used for nonsolvent peaks. However, peaks originating from ion pairs were allowed less broadening than other anionic peaks. The Gaussian broadening was, however, never allowed to be less than the instrumental broadening. The instrumental Gaussian broadening for Raman was measured at 0 cm^{-1} and was found to be 1.5 cm^{-1}. For IR, a Gaussian bandwidth minimum of 2.0 cm^{-1} was used.

Computational. An initial geometry optimization for the anion was made using ab initio Hartree−Fock (HF) self-consistent field molecular orbital methods employing the standard 3-21G* basis set. The search for stable lithium cation positions relative to the anion was performed by choosing six different starting points in the plane of the anion and one above the ring plane for geometry optimizations (HF/3-21G*). The search resulted in four different stable positions for the lithium ion (Figure 2a−d). These structures and the anion structure were

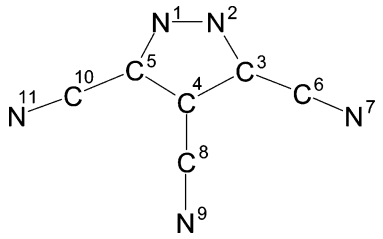

Figure 1. PATC anion.

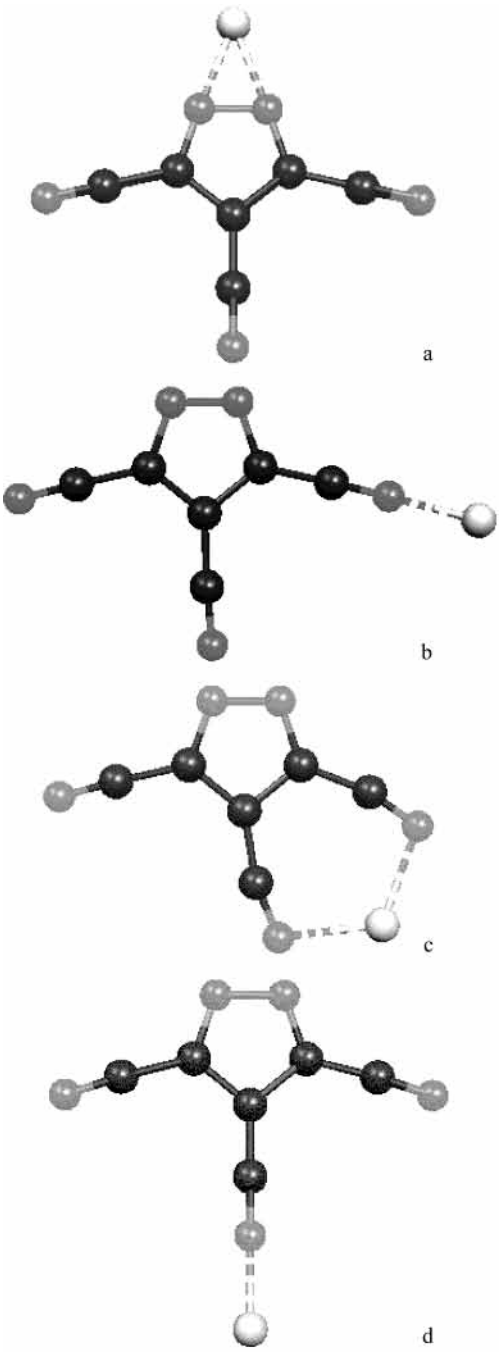

Figure 2. Ion pair structures. (a) Bi1 (C_{2v}). (b) M1 (C_s). (c) Bi2 (C_s). (d) M2 (C_{2v}).

further optimized at the HF/6-31G* level followed by HF/Sadlej-pVTZ.[16−18]

Vibrational frequency calculations were performed for all stable structures to determine whether the structures were local minima and to get theoretical IR and Raman spectra. The Sadlej-

TABLE 1: Selected Geometry Parameters for the Anion and the Ion Pairs (HF/Sadlej-pVTZ)

bond length (Å)	anion		ion pairs			
	(C_{2v})	(HF/6-31G*)	Bi1 (C_{2v})	M1 (C_s)	Bi2 (C_s)	M2 (C_{2v})
r(N1−N2)	1.313	1.311	1.329	1.294	1.317	1.331
r(N1−C5)	1.326	1.327	1.317	1.340	1.324	1.307
r(N2−C3)	1.326	1.327	1.317	1.335	1.312	1.307
r(C5−C4)	1.396	1.396	1.393	1.383	1.392	1.407
r(C3−C4)	1.396	1.396	1.393	1.400	1.403	1.407
r(C5−C10)	1.437	1.435	1.437	1.436	1.437	1.438
r(C3−C6)	1.437	1.435	1.437	1.409	1.429	1.438
r(C4−C8)	1.425	1.424	1.429	1.427	1.412	1.393
r(C10−N11)	1.136	1.138	1.133	1.134	1.134	1.135
r(C6−N7)	1.136	1.138	1.133	1.139	1.140	1.135
r(C8−N9)	1.137	1.139	1.134	1.136	1.142	1.142
r(Li−N1)			1.857			
r(Li−N2)			1.857			
r(Li−N7)				1.804	2.033	
r(Li−N9)					2.016	1.802

pVTZ basis set was chosen for these calculations as it is designed to give a good description of polarizability changes and thus better theoretical Raman intensities. The obtained frequencies (HF/Sadlej-pVTZ) are scaled by 0.8981 for frequencies below 1800 cm^{-1} and 0.9097 for frequencies above 1800 cm^{-1}.[19] Some Raman intensity values for the ion pairs were unreasonably high: ∼19 000 Å^4·amu. Additional vibrational frequency calculations were, therefore, performed for all structures using the 6-31G* basis set. However, all IR intensities were reasonable for all structures, as were all Raman intensities for the pure anion.

The DMSO spectra were also calculated ab initio using the same methods as for the salt in order to simplify the peak fitting analysis. The regions where DMSO peaks influence the anionic peaks of the salt solutions are 300−400, 650−700, 900−1060, and 1280−1440 cm^{-1}.

Visualization of the different vibrational modes was done using the program Molekel.[20]

Lithium ion binding energies were calculated as the differences in electronic energies: $\Delta E_{\text{bind}x} = E_{(\text{ion-pair})} - \sum(E_{(\text{Li}^+)} + E_{(\text{anion}x)})$, where $E_{(\text{anion}x)}$ is the energy for the free anion ($x = 1$) and the ion pair anion ($x = 2$) geometry, respectively. The difference in energy, ΔE, between the different ion pairs was calculated for all basis sets. A zero-point energy (zPE) correction has been applied to all stable structures.

Mulliken and Löwdin analysis was done on HF/6-31G* and HF/Sadlej-pVTZ levels for the anion.

Initial calculations (HF/3-21G*) were made using the Gaussian 98 program;[21] all other calculations were made using the GAMESS program.[22]

Results and Discussion

Anion: Geometry and Charge Distribution. Selected geometry parameters and the charge distribution for the anion are presented in Tables 1 and 2, respectively. The symmetry of the anion is C_{2v} (Figure 1).

The bonding situation can be estimated by comparing obtained bond lengths with standard bond lengths given in a reference table.[23] The N^1-N^2 bond is found to be longer than a standard double bond by ∼0.06 Å, the C−N bonds within the ring are ∼0.03 Å longer than standard double bonds, and the C−C ring bonds are the same length as standard benzene ring bonds. The C−C bonds attaching the CN groups to the ring are also conjugated bonds with a bond length ∼0.03 Å longer than a benzene carbon bond and thus significantly shorter than single bonds. Thus, all ring atoms and the carbon atoms attached to the ring are part of a heavily conjugated system.

TABLE 2: Atomic Charges for the PATC and the TADC Anion (HF/6-31G*)

atom	Mulliken		Löwdin	
	PATC	TADC[9]	PATC	PATC(HF/Sadlej-pVTZ)
N1	−0.37	−0.15	−0.17	−0.20
N2		−0.35		
C1	+0.24	+0.08	−0.036	−0.085
C2	−0.12		−0.11	−0.087
C(CN1)	+0.30	+0.29	+0.026	+0.019
C(CN2)	+0.27		+0.022	−0.013
N(CN1)	−0.50	−0.45	−0.18	−0.12
N(CN2)	−0.49		−0.19	−0.12
$\sum_{\text{ring}}$	−0.38	−0.69	−0.52	−0.66
$\sum_{\text{CN}}$	−0.62	−0.32	−0.48	−0.34

All three C−N bonds of the pending CN groups are ∼0.02 Å shorter than regular C−N triple bonds. The bond lengths in the PATC are similar (within 0.001 Å) to the bond lengths in the TADC.[9] Where there are discrepancies, the bond lengths in PATC are always longer than those in TADC.

The relative electron-withdrawing power of the CN groups can be estimated by comparing with our previously reported results for the TADC anion.[9] In the PATC anion, the three CN groups withdraw 0.62e charge from the ring. In the TADC anion, the total charge withdrawn by the two CN groups is 0.32e. As a result, the PATC anion ring is significantly more positive. However, in the PATC anion, the charge of two neighboring nitrogen atoms is −0.74e compared with −0.50e for the TADC anion. This suggests that locally the negative charge exposed to an approaching lithium ion is larger for the PATC anion. Thus, the present binding-energy results (below) must be interpreted as due to an extensive conjugation in the anions that makes the total ring charge (−0.38e for PATC vs −0.68e for TADC) the more important factor in determining the strength of the lithium ion−anion interaction.

Ion Pairs: Geometries and Binding Energies. The four stable structures of the 1:1 ion pairs, all planar, are shown in Figure 2a−d. Selected geometry parameters are presented in Table 1. The most stable lithium complex, for all calculation levels, was the bidentate lithium ion (Bi1) coordination to the two nitrogen atoms in the ring. The total energy (HF/6-31G*) when the lithium ion coordinates to two CN groups (Bi2) was 44 kJ mol^{-1} higher, and for monodentate (M) coordination to the CN groups, the total energy was ∼85 kJ mol^{-1} higher (Figure 2a−d, Table 3). All four structures were true minima; no imaginary frequencies were found. The energy differences between the different structures suggest that the coordination of Li^+ to the ring nitrogen atoms is the dominating ion pair at room temperature. Also, in the previous study of Li(TADC), a preferred lithium ion coordination to two ring nitrogen atoms was obtained.[9]

The lithium ion binding energy ($\Delta E_{\text{bind}x=1}$, HF/6-31G*) for the most stable structure is ∼530 kJ mol^{-1}, which is lower than the corresponding energy (∼550 kJ mol^{-1}) for its relative Li(TADC). This means that introducing one extra electron-withdrawing CN group gives a more dissociated lithium salt. The lithium ion binding energy is also lower compared to that of other types of lithium salts considered for solid polymer electrolytes (e.g., LiTFSI, ∼630 kJ mol^{-1} and $LiPF_6$, ∼645 kJ mol^{-1}).[24]

Vibrational Analysis. Since the PATC anion has a very low lithium ion affinity, the signals arising from ion pairs in the spectra of the lower concentrations (1.6−2.4 M) are weak, and clear ion pair signals are found only for the saturated

TABLE 3: Total, Relative, and Binding Energies for the Ion Pairs

complex	basis set	energy (au)	zPE (au)	energy[a] (au)	ΔE^a (kJ·mol^{-1})	$\Delta E_{bind1}{}^b$ (kJ·mol^{-1})	$\Delta E_{bind1}{}^{a,b}$ (kJ·mol^{-1})	ΔE_{bind2} (kJ·mol^{-1})
Bi1 (C_{2v})	6-31G*	−506.910354	0.061631	−506.848723	0	−529	−522	−532
	Sadlej-pVTZ	−507.009710	0.061589	−506.948121	0	−551	−543	−627
Bi2 (C_s)	6-31G*	−506.893045	0.061160	−506.831885	44	−484	−478	−520
	Sadlej-pVTZ	−506.993476	0.060838	−506.932638	41	−508	−502	−577
M1 (C_s)	6-31G*	−506.874796	0.060678	−506.814118	91	−436	−432	−440
	Sadlej-pVTZ	−506.979333	0.061186	−506.918148	79	−471	−464	−475
M2 (C_{2v})	6-31G*	−506.877119	0.060715	−506.816404	85	−442	−438	−448
	Sadlej-pVTZ	−506.980804	0.061009	−506.919795	74	−475	−469	−481

[a] zPE correction has been applied. [b] E_{anion} = −499.473404 (zPE = 0.059062); −499.591972 (zPE = 0.058644) au. E_{Li^+} = −7.235536; −7.208061 au.

solution. The assignments made in Table 4 are based on calculated vibrational frequencies, IR and Raman intensities, visualization of the modes, symmetry, and the experimental spectra, both IR and Raman.

The symmetry of the anion is C_{2v}, and we expect $10A_1 + 3A_2 + 9B_1 + 5B_2$ modes, 27 in total. The frequencies and intensities from the calculations on the anion were in good agreement with the experimentally observed frequencies and intensities; a 1:1 ratio was found in spectra from unsaturated solutions with only one exception, modes 21 and 22 having switched places with respect to the computed values.

Given the large energy difference between the different ion pairs, $\Delta E = 40-90$ kJ mol^{-1}, the most stable ion pair is assumed to be the only existing ion pair, and thus we investigate the agreement between calculations and experiments for this case. The symmetry for the ion pair is C_{2v}, the same as that for the anion, and the three additional modes, $2B_2$ and $1A_1$, are found for the ion pair. Of the other ion pairs found by calculation, two have C_s (Figure 2b and c) and one has C_{2v} symmetry (Figure 2d).

In the most stable ion pair, the lithium ion is coordinated to the ring nitrogen atoms, whereas in the other three the lithium ion is coordinated to CN groups. Thus, it is probably possible to determine if ion pairing to the ring atoms or the CN groups exists just by analyzing the CN stretching region, 2200−2300 cm^{-1} (Figure 3a and b). Further differences are expected in the ring vibration region, 1000−1500 cm^{-1} (Figure 4). Another approach is to investigate the lithium ion−anion vibrations that appear between 120 and 500 cm^{-1} (Figure 5). In this region, however, only Raman spectra are available because the lower limit of the ATR unit used for recording IR spectra is ∼625 cm^{-1}.

There are three different CN stretches. The calculations showed that two are strong in Raman and weak in IR and vice versa for the third. However, the bands are separated by only about 10 cm^{-1}. Two main peaks were clearly seen in the Raman spectra of unsaturated solutions at 2225 and 2235 cm^{-1}, the latter being the strongest. In IR, one main peak was seen at 2229 cm^{-1}, with a shoulder at 2225 cm^{-1}. The main IR peak is thus the out-of-phase stretch of the outer CN groups (mode 26, Table 4). The relative intensities correspond well to the calculated values.

In the Raman spectrum of the saturated solution, two main peaks are found at 2236 and 2240 cm^{-1}; additionally, a shoulder is found at 2225 cm^{-1}. The two strong peaks are lithium ion-influenced CN stretches, modes 25 and 27. These correspond well to calculated positions as the two strong Raman peaks (modes 25 and 27) should be shifted to higher frequencies by 37 and 31 cm^{-1}, respectively. The experimentally found shifts were smaller, 11 and 6 cm^{-1}, respectively. This is reasonable because calculations often overestimate frequency shifts in ionic compounds, as, for example, in this case when the lithium ion's surroundings have been neglected.[24] In the IR spectrum of the saturated solution, the influence of ion pairing is not as visible as in Raman. However, a shoulder can clearly be seen on the main peak at 2238 cm^{-1}, which is the corresponding ion pair mode. By adding an ion pair peak at 2236 cm^{-1} (mode 25), the peak fit improves, resulting in excellent agreement with the Raman data. Thus, the corresponding ion pair vibrations follow the same frequency order as the pure anion vibrations.

There are seven anion modes in the ring-stretching region (Figure 4). Several of these have high intensities in Raman, whereas in IR the only strong band not influenced by solvent is the one at 1492 cm^{-1}. The 1492-cm^{-1} band is strong in both IR and Raman and is assigned to an in-phase stretch of the ring carbon atoms. Between 1100 and 1200 cm^{-1}, there are two clearly visible bands, one strong in Raman (1120 cm^{-1}) and one visible in IR (1184 cm^{-1}). The peak at 1321 cm^{-1} that is strong in Raman is assigned to the ring breathing mode (mode 22), although the calculated frequencies suggest it to be mode 21. However, the theoretical intensities (both IR and Raman) strongly support this assignment.

In the Raman spectra of the saturated solution, three very strong and narrow peaks were found at 1159, 1349, and 1502 cm^{-1}. These three peaks, along with additional smaller peaks, all correspond well to the calculations of the corresponding ion pair modes.

Out of the three additional ion pair modes (Li1-3, Table 4), the mode with the theoretically highest frequency should appear at ∼500 cm^{-1} and therefore should be clearly visible in the Raman spectrum of the saturated solution. The calculated anion modes between 400 and 550 cm^{-1} could easily be fit to the spectra from the unsaturated solutions. In the 4.0 M solution spectrum, two pronounced changes are observed: the peaks at 520 cm^{-1} are sharper and more intense, as predicted by calculations of the corresponding ion pair peaks, and a new sharp peak is seen at 471 cm^{-1}, tentatively assigned to the symmetric in-plane $Li^+-N^{1,2}$ stretch.

The other two additional ion pair modes have calculated frequencies of 124 and 170 cm^{-1}, respectively. Analysis at such low frequencies is difficult, but these modes are probably the Raman peaks seen in the spectrum collected for the saturated solution at 147 and 200 cm^{-1}, respectively. These modes are not visible in the spectra recorded for the lower-concentration samples.

The present calculations showed possibilities for three other ion pairs, all, however, with higher total energies. No traces of any of these ion pairs are detected in the spectra. As the lithium ion in all of these ion pairs is coordinated to CN groups, the most pronounced differences would be found in the CN

TABLE 4: Calculated and Measured Vibrational Frequencies, IR and Raman Intensities, Symmetries, and Mode Assignments

	calculated						experimental[c]					
	anion	ion pair		intensities				intensities[b]				
mode	ν_{scaled} (cm^{-1})	ν_{scaled} (cm^{-1})	$\Delta\nu$ (cm^{-1})	Raman[a] ($Å^4$·amu^{-1})	IR ($km·mol^{-1}$)	sym (C_{2v})	ν (cm^{-1})	Raman 1.6 M	IR 1.6 M	Raman 4.0 M	IR 4.0 M	assignment[d]
1	81		+1	0.11	1.8	B_2	80					$\tau^{o.o.pl.}$ $N^{2,1}-C^{3,5}-C^{6.10}-N^{7.11}$
		80		0.0	13	B_2						
2	105		−7	4.7	0.51	B_1	112					$\tau^{i.pl.}$ $C^{3,5}-C^4$-C^8-N^9
		102		5.5	3.1	B_1						
3	121		0	1.0	5.9	A_1	121					$\tau^{i.pl.}$ $N^{2,1}-C^{3,5}-C^{6,10}-N^{7,11}$
		117	−3	45.3(1.2)	11	A_1	120					
Li1		124	−23	0.23	14	B_2	147			2.0		$\nu^{o.o.pl.}$ Li− $N^{1,2}$
Li2		170	−30	0.86	27	B_1	200			1.3		$\nu_{as}^{i.pl.}$ Li−$N^{1,2}$
4	179		−1	0.0	20	B_2	180					$\tau^{o.o.pl.\ i.ph.}$ $C^{3,5}-C^4-C^8-N^9$
		225		0.0	58	B_2						
5	222		−13	2.5	0.0	A_2	235	0.080		0.10		$\tau^{o.o.pl.}$ $C^5-N^1-N^2-C^3$
		227	−11	0.17	0.0	A_2	238			0.18		
6	249			0.43	16	B_1						i.pl. ring rotation + $\delta^{i.pl\ i.ph.}$ $C^{3,5}-C^{6,10}-N^{7,11}$
		274		0.0	48	B_1						
7	442		0	2.5	0.034	A_1	442	0.040		0.024		$\delta^{i.pl.\ i.ph.}$ $N^{2,1}-C^{3,5}-C^4$
		440	+3	630(3.4)	5.9	A_1	437			0.24		
8	467		+5	0.26	7.6	B_2	462	0.58		0.53		$\delta^{o.o.pl.\ i.ph.}$ $C^{3,5}-C^{6,10}-N^{7,11}$ + $\delta^{o.o.pl.}$ $C^4-C^8-N^9$
		446		0.19	8.9	B_2						
9	486		+12	3.1	13	A_1	474	0.43		0.66		$\delta^{i.pl.\ i.ph.}$ $C^{3,5}-C^{6,10}-N^{7,11}$
		473	+7	2000(4.0)	26	A_1	466			0.34		
10	493		+4	6.9	4.6	B_1	489	0.60		0.74		$\delta^{i.pl.}$ $C^4-C^8-N^9$
		477	−6	7.8	0.46	B_1	483			0.75		
Li3		502	+31	44(6.5)	114	A_1	471			0.78		$\nu_s^{i.pl}$ Li−$N^{1,2}$
11	546		+23	5.6	0.0	A_2	523	0.71		1.2		$\delta^{o.o.pl.\ o.o.ph.}$ $C^{3,5}-C^{6,10}-N^{7,11}$
		542	+20	6.1	0.0	A_2	522			1.0		
12	546		+25	2.4	19	B_2	521	0.46		0.56		$\delta^{o.o.pl.\ i.ph.}$ $C^{3,4,5}-C^{6,8,10}-N^{7,9,11}$
		539	+22	3.12	7.2	B_2	517			0.29		
13	612		+3	0.18	1.5	B_1	609	0.020		0.020		$\delta^{i.pl.\ o.o.ph.}$ $N^{1,2}-C^{5,3}-C^{10,6}$
		620	+3	0.58	5.9	B_1	617			0.020		
14	624		−21	0.55	8.0	A_1	645	1.3	1.3	1.2	4.3	$\nu^{i.pl.\ i.ph.}$ C^4-C^8 + $\nu^{i.pl.\ i.ph.}$ $N^{1,2}-C^{5,3}$
		663	+5	58(1.2)	98	A_1	658			2.0	4.7	
15	703		+28	2.5	0.0	A_2	675	7.7	1.2	14	2.4	$\delta^{o.o.pl.}$ $C^{3,5}-N^{2,1}-N^{1,2}$
		722	+38	3.9	0.0	A_2	684			4.0		
16	715		+6	1.1	1.2	B_2	709	3.8	7.7	7.0	12	$\delta^{o.o.pl.}$ $C^3-C^4-C^5$
		757	+43	1.1	2.7	B_2	714			2.2	1.8	
17	725		−17	1.6	0.17	B_1	742	0.19	1.0	0.20	1.8	$\delta^{i.pl.\ o.o.ph}$ $C^{6,10}-C^{3,5}-C^4$ + $\delta^{i.pl.}$ $C^{3,5}-C^4$-C^8
		730	−23	1.9	0.0	B_1	753			0.13	0.71	
18	1015		−15	3.5	28	B_1	1030	0.49	23	0.57	32	$\nu^{i.pl.\ o.o.ph.}$ N^1-N^2
		1031	−24	0.25	20	B_1	1055			0.83	4.2	
19	1157		+37	221	3.7	A_1	1120	6.4	0.034	4.1	0.15	$\nu^{i.pl.\ i.ph.}$ N^1-N^2
		1143	−16	66(31)	27	A_1	1159			5.0	0.31	
20	1170		−15	5.6	21	A_1	1185	0.66	1.3	0.41	2.6	$\nu^{i.pl.\ i.ph.}$ $N^{1,2}-C^{5,3}$ + $\nu^{i.pl.}$ i.ph. C^4-C^8
		1198	+1	4.8(0.8)	23	A_1	1197			0.42	0.10	
21	1324		−11	23	0.39	B_1	1335	0.90	0.30	2.0	1.1	$\nu^{i.pl.\ o.o.ph.}$ $N^{1,2}-C^{5,3}$ + $\nu^{i.pl.\ o.o.ph.}$ $C^{3,5}-C^4$
		1303	−9	72	14	B_1	1312			0.90	5.2	
22	1335		+14	148	28	A_1	1321	7.7	5.4	6.0	10	ring breathing mode
		1408	+60	120(140)	63	A_1	1348	0.090		13	2.7	
23	1426		+10	7.2	5.1	B_1	1416	1.1	4.9	1.3	8.0	$\nu^{i.pl.\ o.o.ph.}$ $C^{3,5}-C^4$
		1470	+22	2.6	15	B_1	1448			0.60	1.2	
24	1480		−12	90(60)	48	A_1	1492	3.4	9.2	2.8	16	$\nu^{i.pl.\ i.ph.}$$C^{3,5}-C^4$
		1495	−6	64(44)	34	A_1	1501	0.10	0.20	5.0	2.3	
							2218	1.3	0.60	2.7	4.1	isotope shift (^{13}C) of mode 27
25	2322		+97	220(220)	140	A_1	2225	10	13	9.3	19	$\nu^{i.pl.}$ C^8-N^9
		2359	+123	19000(200)	63	A_1	2236	0.48		11	5.8	
26	2330		+100	17(17)	277	B_1	2230	2.1	39	2.8	56	$\nu^{i.pl.\ o.o.ph.}$ $C^{6,10}-N^{7,11}$
		2366	+128	15(16)	55	B_1	2238				4.0	
27	2336		+101	820(630)	25	A_1	2235	13	2.4	16	6.0	$\nu^{i.pl.\ i.ph.}$ $C^{6,10}-N^{7,11}$
		2367	+126	2900(480)	2.1	A_1	2241	0.77		24		

[a] Values in parentheses are from the HF/6-31G* calculations. [b] The intensities are scaled with the DMSO C−H stretch at ∼3000 cm^{-1}. [c] In the region below 200 cm^{-1}, there has been only approximate peak fitting of the Li1−2 modes, and for the remaining modes, only the positions, without area calculations, are presented. [d] o.o.pl. − out of plane, i.pl. − in plane, o.o.ph. − out of phase, i.ph. − in phase.

stretching region. The calculations show that the CN modes for these three ion pairs should be very different from the corresponding CN modes for the free anion. This was not seen experimentally, where the shifts are very uniform (11, 8, and 6 cm^{-1}), which is also the case for the calculated shifts for the most stable ion pair (37, 36, and 31 cm^{-1}). In contrast, the calculated shifts for the other three ion pairs are very inhomogeneous: −38, 10, and 18 cm^{-1} for two of them and −54, 20,

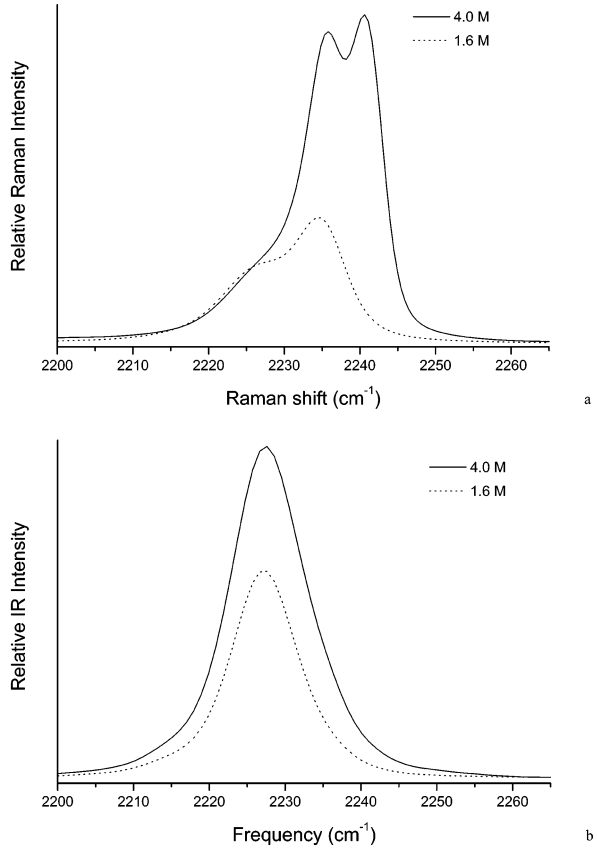

Figure 3. (a) Raman and (b) IR spectra of the CN stretching region.

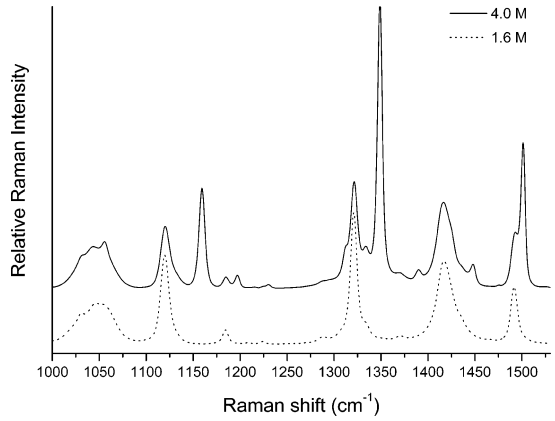

Figure 4. Raman spectrum of the ring vibration region.

and 17 cm^{-1} for the third. This difference in shift directions in the CN modes for these three ion pairs should result in a large separation that should be clearly visible experimentally if these ion pairs were present because the calculated intensities are high. This strongly indicates that the only experimentally observed ion pair is ring-coordinated. The three lithium ion−anion vibrations also indicate that ring coordination is the only existing coordination.

Conclusions

In solution, the lithium ion has bidentate coordination to the ring nitrogen atoms. This conclusion is supported by the calculated binding energies and a vibrational analysis. Introducing a third carbonitrile group to the azole ring resulted in a more dissociated salt, as determined by the lithium binding energies that are lower for this anion than for its relative, the TADC anion. The lithium affinities are also lower by ∼20% than for most other simple inorganic anions, making it a possible choice for polymer and liquid electrolyte purposes and other applications where weakly basic anions are required. Using this salt may also open other possibilities for choosing other polymer matrices and thus gaining higher total conductivities as well as cation transport numbers in polymer battery applications.

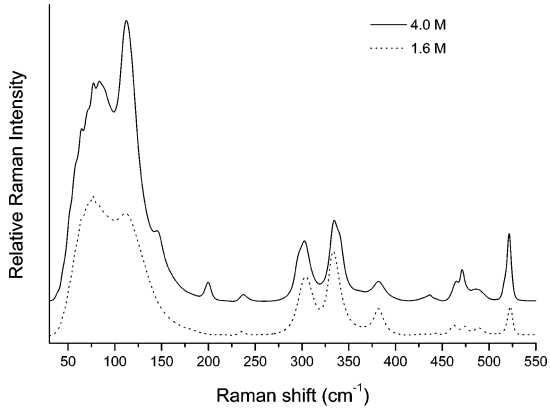

Figure 5. Raman spectrum of the lithium ion−anion stretching region.

Acknowledgment. This work was supported with grants from the Nordic Energy Research Program (NERP), the Swedish Research Council (VR), and by the Centre National de la Recherche Scientifique (CNRS).

Supporting Information Available: Selection of DMSO modes, calculated and experimental. This material is available free of charge via the Internet at http://pubs.acs.org.

Note Added after ASAP Posting. This article was released ASAP on 11/01/2003. The author running head has been changed from Nilsson et al. to Markusson et al. The correct version was posted on 11/06/2003.

References and Notes

(1) MacCallum, J. R.; Vincent, C. A. *Polymer Electrolyte Reviews*; Elsevier Applied Science: London, 1987; Vol. 1.
(2) Frech, R.; Huang, W. J. *Solution Chem.* **1994**, *23*, 469.
(3) Ma, Y.; Doyle, M.; Fuller, T. F.; Doeff, M. M.; De Jonghe, L. C.; Newman, J. *J. Electrochem. Soc.* **1995**, *142*, 1859.
(4) Klassen, B.; Aroca, R.; Nazri, G. A. *J. Phys. Chem.* **1996**, *100*, 9334.
(5) Huang, W.; Frech, R.; Wheeler, R. A. *J. Phys. Chem.* **1994**, *98*, 100.
(6) Johansson, P. *J. Phys. Chem. A* **2001**, *105*, 9258.
(7) Tullo, A. *Chem. Eng. News* **2000**, *78* (21), 9.
(8) Tullo, A. *Chem. Eng. News* **2000**, *78* (22), 12.
(9) Johansson, P.; Béranger, S.; Armand, M.; Nilsson, H.; Jacobsson, P. *Solid State Ionics* **2003**, *156*, 129.
(10) Michot, C. Ph.D. Thesis, Institut National Polythechnique de Grenoble, Canada, 1995.
(11) Billes, F.; Endrédi, H.; Jalsovszky, G. *J. Mol. Struct.* **1999**, *465*, 157.
(12) Orza, J. M.; García, M. V.; Alkorta, I.; Elguero, J. *Spectrochim. Acta, Part A* **2000**, *56*, 1469.
(13) Weis, C. D. *J. Org. Chem.* **1962**, *27*, 3695.
(14) Dewar, M. J. S.; Pettit, R. *J. Chem. Soc.* **1956**, 2026.
(15) *PeakFit*, v4.04 Win32 ed.; AISN Software Inc.: 1995.
(16) http://www.emsl.pnl.gov:2080/forms/basisform.html. Accessed 09-14-2002.
(17) Sadlej, A. J. *Collect. Czech. Chem. Commun.* **1988**, *53*, 1995.
(18) Sadlej, A. J. *Theor. Chim. Acta* **1992**, *79*, 123.
(19) Halls, M. D.; Velkovski, J.; Schlegel, H. B. *Theor. Chem. Acc.* **2001**, *105*, 413.
(20) Flükiger, P.; Lüthi, H. P.; Portmann, S.; Weber, J. *MOLEKEL*, 4.0 ed.; Swiss Center for Scientific Computing: Manno, Switzerland, 2000.
(21) Frisch, M. J.; Trucks, G. W.; Schlegel, H. B.; Scuseria, G. E.; Robb, M. A.; Cheeseman, J. R.; Zakrzewski, V. G.; Montgomery, J. A., Jr.;

Stratmann, R. E.; Burant, J. C.; Dapprich, S.; Millam, J. M.; Daniels, A. D.; Kudin, K. N.; Strain, M. C.; Farkas, O.; Tomasi, J.; Barone, V.; Cossi, M.; Cammi, R.; Mennucci, B.; Pomelli, C.; Adamo, C.; Clifford, S.; Ochterski, J.; Petersson, G. A.; Ayala, P. Y.; Cui, Q.; Morokuma, K.; Malick, D. K.; Rabuck, A. D.; Raghavachari, K.; Foresman, J. B.; Cioslowski, J.; Ortiz, J. V.; Stefanov, B. B.; Liu, G.; Liashenko, A.; Piskorz, P.; Komaromi, I.; Gomperts, R.; Martin, R. L.; Fox, D. J.; Keith, T.; Al-Laham, M. A.;Peng, C. Y.; Nanayakkara, A.; Gonzalez, C.; Challacombe, M.; Gill, P. M. W.; Johnson, B. G.; Chen, W.; Wong, M. W.; Andres, J. L.; Head-Gordon, M.; Replogle, E. S.; Pople, J. A. *Gaussian 98*, revision A.9; Gaussian, Inc.: Pittsburgh, PA, 1998.

(22) Schmidt, M. W.; Baldridge, K. K.; Boatz, J. A.; Elbert, S. T.; Gordon, M. S.; Jensen, J. H.; Koseki, S.; Matsunaga, N.; Nguyen, K. A.; Su, S.; Windus, T. L.; Dupuis, M.; Montgomery, J. A., Jr. *J. Comput. Chem.* **1993**, *14*, 1347.

(23) Aylward, G. H.; Findlay, T. *SI Chemical Data*, 5th ed.; Wiley: New York, 2002.

(24) Johansson, P.; Jacobsson, P. *J. Phys. Chem. A* **2001**, *105*, 8504.